On the investigation of thermal/cooling-gel biphasic systems based on hydroxypropyl methylcellulose and hydroxypropyl starch

Yanfei Wang[a,b,c], Long Yu[b,*], Fengwei Xie[d,e,f,†], Sheng Li[c], Qingjie Sun[a], Hongsheng Liu[b], Ling Chen[b]

[a] *College of Food Science and Engineering, Qingdao Agricultural University, Qingdao, Shandong 266109, China*

[b] *College of Food Science and Engineering, South China University of Technology, Guangzhou, Guangdong 510640, China*

[c] *CSIRO, Manufacturing Flagship, Bayview Avenue, Clayton, Vic 3168, Australia*

[d] *Institute of Advanced Study, University of Warwick, Coventry CV4 7HS, United Kingdom*

[e] *International Institute for Nanocomposites Manufacturing (IINM), WMG, University of Warwick, Coventry CV4 7AL, United Kingdom*

[f] *School of Chemical Engineering, The University of Queensland, Brisbane, Qld 4072, Australia*

[*] Corresponding author. *E-mail address*: felyu@scut.edu.cn (L. Yu),

[†] Corresponding author. *E-mail addresses*: f.xie@uq.edu.au; fwhsieh@gmail.com (F. Xie)

Abstract

This work investigates the rheology, structure, and properties of novel thermal/cooling-gel biphasic systems formed by hybridization of hydroxypropyl methylcellulose (HPMC) as a thermal gel and hydroxypropyl starch (HPS) as a cooling gel. Due to the different gelation properties, HPS became the dispersed phase in the other continuous phase at low temperatures, and so did HPMC at high temperatures. However, the dispersed phase could play a dominant role in the viscosity, thixotropy, and gel properties of the blends, and subsequently affect the crystalline structure, fractal structure, mechanical properties, oxygen permeability, and thermal stability of the blend films. Moreover, the rheological properties and the film structure and performance could also be varied by the chemical modification of starch. Hydroxypropylation could break the starch intermolecular hydrogen bonding, disrupt its ordered structure, inhibit the molecular rearrangement, and result in a softer gel texture that was more compatible with HPMC. With a higher degree of hydroxypropyl substitution, the resultant blend films were more amorphous and flexible but exhibited decreased mechanical properties and oxygen permeability. The knowledge obtained from this work could provide guidance to further developing various thermal/cooling-gel multi-phasic systems with desired properties and functionality.

Keywords: hydroxypropyl methylcellulose; hydroxypropyl starch; rheological properties; films; mechanical properties; oxygen barrier property

1 Introduction

The blending of two or more polymers has been considered as one of the most cost-effective methods to modify the bulk properties of individual polymers, achieve enhanced and/or new material properties, reduce costs, and to expand the applications of polymer materials (Taguet et al., 2014; Wang et al., 2016a; Wang et al., 2016b).

Hydroxypropyl methylcellulose (HPMC), a derivative of cellulose, the richest natural polymer on the Earth, has good water solubility and biodegradability, and excellent film-forming, mechanical and barrier properties. Therefore, HPMC has been extensively used in food packaging, medicinal capsules, and other drug delivery systems (Imran et al., 2014; Zhang et al., 2017a; Zhang et al., 2015; Zhang et al., 2017b). However, the high prices of HPMC limit its general applications, even for use in therapeutic delivery systems (Wang et al., 2016a; Wang et al., 2016b; Zhang et al., 2013b; Zhang et al., 2013c). Regarding this, starch, which is widely used in food industry, can be a cheap material to decrease the price of HPMC. Native starch is a storage carbohydrate of plants and usually modified by chemical or physical methods to improve its processability and properties and to widen its applications (Adak and Banerjee, 2016; Lee and Yoo, 2011; Luallen, 2004; Masina et al., 2017). Hydroxypropyl starch (HPS) is a typical chemically modified starch and is an inexpensive material being widely used in the food industry (Wang et al., 2016a; Zhang et al., 2015). Therefore, the commercial potential of HPMC/HPS is foreseeable for a broad range of applications such as food packaging, food, and medicines.

Edible materials from natural polymers can be easily produced via a wet process (Cuq et al., 1998). It is based on a film-forming solution or dispersion where polymers are first solubilized or dispersed into a liquid phase, which is then concentrated with the removal of the liquid (usually by drying at a higher temperature). This process is generally preferred to form edible pre-formed films, or to apply coatings in the liquid form directly onto products by dipping, brushing, or spraying. The design of processes for such materials requires accurate data regarding the rheological properties of

64 film-forming solutions or dispersions, which play an important role in controlling the defects in the
65 thin films after coating (Peressini et al., 2003).
66 It is well known that both HPMC and HPS can form hydrogels, but their gelation behaviors are
67 quite different. HPMC is a thermal gel that forms a hydrogel at a higher temperature and its gel
68 disaggregates at a lower temperature, which is distinctly different from the conventional hydrogels
69 such as gelatin (Dhillon and Seetharaman, 2011; Haque et al., 1993; Liu et al., 2008). The widely-
70 accepted gelation mechanism of HPMC regards the intermolecular association of hydrophobic
71 groups on the polymer chains, leading to crosslinking and gel formation (Haque and Morris, 1993;
72 Haque et al., 1993; Li, 2002; Viriden et al., 2010). As the film-forming solutions need to be dried at a
73 higher temperature, the thermal-gelation property can cause much difficulty in fabricating HPMC
74 films. Regarding this issue, HPS has shown to be able to decrease the gelation point of HPMC since
75 it has a cooling-gelation property (Zhang et al., 2015). The mechanism of the gelation of HPS relates
76 to the formation of a three-dimensional network by interchain hydrogen bonding during the cooling
77 process. Meanwhile, research has shown that HPMC can also influence the gelation property of
78 starch (Correa et al., 2010; Kadokawa et al., 2009; Rosell et al., 2011). Therefore, for practical
79 applications, it is fundamentally important to thoroughly understand the gelation and rheological
80 properties of the thermal/cooling-gel bi-phasic systems based on HPMC/HPS.
81 It is known that a small change in chemical structure of starch can result in dramatic changes in
82 their rheological properties. Thus, chemical modification further provides the possibilities to improve
83 and control the rheological properties of the final bi-phasic systems involving starch (Chun and Yoo,
84 2007). In turn, the understanding of the changes in rheological properties of starch caused by
85 chemical modification is helpful in understanding the structural properties and can also assist in the
86 design of modified starches with improved properties (Lee and Yoo, 2011). HPS is generally
87 prepared by etherification of native starch with propylene oxide in the presence of an alkaline
88 catalyst. The hydroxypropyl groups are hydrophilic in nature. When these groups are introduced onto

the starch chains, they weaken or disrupt the internal hydrogen bonding that maintains the whole granule structure. Therefore, the physicochemical properties of starch could be influenced by hydroxypropylation depending on the molar substitution (MS) (Lee and Yoo, 2011; Moin et al., 2017; Schmitz et al., 2006; Woggum et al., 2015).

While the physicochemical properties of HPS with different MS has been concerned in many studies (Han et al., 2005; Kaur et al., 2004; Lawal et al., 2008; Schmitz et al., 2006), much less attention (Chun and Yoo, 2007; Lee and Yoo, 2011; Ren et al., 2017) has been paid to the rheological and gel properties of HPS, as well as the material structure properties of the blends that contain HPS. In this work, HPS with different MS was added to HPMC to prepare HPMC/HPS blends. The rheological properties and the film structure and performance of HPMC/HPS blends were examined as a function of MS. The knowledge obtained from this work would be vital to understanding the mechanistic relationship between structural modification and properties of the novel thermal/cooling-gel bi-phasic systems.

2 Materials and method

2.1 Materials

A commercially available pharmaceutical-grade HPMC (HT-E15, from HopeTop Pharmaceutical Company, China: viscosity (2%), 6.3 mPa·s; pH 6.0; methoxyl content on the dry basis, 29%; hydroxypropyl oxygen content on dry basis 8.4%) was used in this work. Three food-grade hydroxypropylated corn starches (G80, A939, and A1081) with different MSs (the average amount of hydroxypropyl per unit mole of glucose) (0, 0.04, and 0.11, respectively) were supplied by Penford (Australia).

2.2 Film preparation

For rheological measurement, solutions of 15 wt.% concentration containing HPMC/HPS of different ratios (100/0, 50/50, 0/100) were prepared. For the preparation of these solutions, HPMC and HPS (dry powder) were firstly mixed. Then, the mixtures were dispersed in hot water (70 °C) with stirring for 30 min to ensure a proper distribution of HPMC in the solutions. Afterwards, the solutions were heated to 95 °C and maintained for 1 h to gelatinize HPS in a water bath. For G80, the solutions were gelatinized in a high-pressure reactor at 1500 psi (103 bar) and 110 °C for 30 min instead, since its gelatinization temperature is higher than 100 °C (Liu et al., 2006). The solutions were cooled down to room temperature to dissolve HPMC under stirring before testing.

For film preparation, solutions of 8 wt.% concentration were added with 2.4% PEG as a plasticizer. Solutions were kept at 70 °C for 40 min with slow continuous stirring before film casting. For film casting, 20 g of solutions were poured onto a Petri dish (15 cm diameter) and then dried at 37 °C. The dry films were peeled off from the dishes and kept under 75% RH at 25 °C for at least three days before further characterization.

2.3 Rheological measurement

The rheological properties of samples were investigated using a Discovery HR-2 rheometer (TA Instruments, New Castle, DE, USA). A parallel-plate geometry (60 mm diameter) with the gap set at 1.0 mm was used for the measurements.

Flow patterns were used to understand the steady rheological properties and thixotropy. At a constant shear treatment, the viscosity of a polymer may vary with time before a stable value could be achieved (Tajuddin et al., 2011). As a result, pre-shearing with a shear rate of 800 s^{-1} at room temperature (25 °C) for 1000 s was performed to ensure all the samples to achieve a stable state before further measurement. Steady rheological properties were tested at 25 °C with shear rate

increased from zero to 1000 s^{-1} for 1 min, then kept at 1000 s^{-1} for 1 min, and finally decreased to zero for another 1 min. The curve of shear stress (τ) vs. shear rate ($\dot{\gamma}$) corresponds to the equation:

$$\tau = K\dot{\gamma}^n \quad (1)$$

From this equation, the fluid consistency index (K) and flow behavior index (n) can be calculated.

Small-amplitude oscillatory shear tests were used to explore the dynamic rheological properties. To obtain the linear range of viscoelasticity, strain sweep measurements were performed from 0.01% to 100% at a frequency of 1 Hz at 25 °C. Temperature sweeps involved heating from 5 °C to 85 °C, holding at 85 °C for 5 min, and then cooling to 5 °C. A heating/cooling rate of 2 °C/min was used. The frequency was set at 1 Hz and the strain at 0.1% (to be in the linear range of viscoelasticity). The sample was placed between the parallel plates, and then a small amount of silicone oil was applied to the periphery of the sample to prevent moisture evaporation. Frequency sweeps from 1 rad/s to 100 rad/s were also performed after isothermal equilibration for 5 min at both 5 °C and 85 °C. The strain was set at 0.1% (to be in the linear range of viscoelasticity). Storage modulus (G'), loss modulus (G''), and tan δ were recorded. The frequency-dependence of G' and G'' can be shown in the following power-law equations:

$$G' = G_0'\omega^{n'} \quad (2)$$

$$G'' = G_0''\omega^{n''} \quad (3)$$

From these equations, the slopes (n' and n'') and intercepts (G_0' and G_0'') of log G'–log ω and log G''–log ω can be calculated.

The thixotropy was probed with three-interval thixotropic tests. The tests were carried out at 25 °C with a low-shear stage with shear rate kept at 1 s^{-1} for 50 s, a high-shear stage with shear rate

kept at 1000 s^{-1} for 20 s, then a structural recovery stage with shear rate kept at 1 s^{-1} for 250 s. The structural recovery ratio (DSR) can be defined by the equation:

$$DSR = \eta_t/\eta \times 100\% \quad (4)$$

Here, η_t is the viscosity in the structural recovery stage at a certain time (t) and η is the final viscosity in the first stage.

2.4 Synchrotron small/wide angle X-ray scattering (SAXS/WAXS)

Synchrotron small/wide-angle X-ray scattering (SAXS/WAXS) measurements were carried out on the SAXS/WAXS beamline (flux, 10^{13} photons per second) at the Australian Synchrotron (Clayton, Vic, Australia) at a wavelength λ = 1.47 Å. The 2D scattering patterns were collected using a Pilatus 1M camera (active area, 169 × 179 mm; and pixel size, 172 × 172 μm). The scatterBrain software was used to acquire the one-dimensional (1D) data from the 2D scattering pattern, and the data in the angular range of $0.015 < q < 0.15$ $Å^{-1}$ and $0.095 < q < 2$ $Å^{-1}$ were used as the SAXS and WAXS pattern, respectively, where $q = 4\pi\sin\theta/\lambda$, in which 2θ is the scattering angle and λ is the X-ray wavelength. All data were normalized, and the background intensity and smeared intensity were removed for further analysis.

2.5 Mechanical properties

Tensile properties were evaluated in accordance with the ASTM D5938 standard using an Instron tensile testing apparatus (5565). Tensile strength (σ_t), elongation at break (ε_b) and Young's modulus (E) were measured at a crosshead speed of 10 mm/min. Seven specimens were tested for each sample and the mean values were reported.

2.6 Oxygen permeability (OP)

Oxygen transmission rates of the films were measured by Mocon OXTRAN® 2/21H Master (MH) and Satellite (SH) systems (Mocon Inc., Minneapolis, MN) according to the ASTM D-3985 standard. The exposure area for testing was 50 cm^2 for each sample.

2.7 Thermogravimetric analysis (TGA)

Thermal stability of the samples was evaluated using a PerkinElmer Pyris 1 TGA system. Samples were heated from 30 °C to 700 °C at 10 °C/min in a nitrogen atmosphere.

3 Results and Discussions

3.1 Rheological properties of film-forming solutions

3.1.1 Steady rheological properties

The pre-shearing carried out before the real shearing test was to ensure the samples to achieve a homogeneous and stable state so that the effect of time could be eliminated. **Fig. 1** shows the effect of shear rate on the viscosity of the HPMC/HPS solution with different MSs of HPS. It can be seen that the viscosity of all the samples decreased with increasing shear rate and showed a shear-thinning behavior. Under shear force, most polymer solutions of high concentrations will undergo significant disentanglement and molecule rearrangement, showing a pseudoplastic behavior (Heyman et al., 2014; Zhang et al., 2015). For pure HPS, the viscosity was higher and the shear-thinning behavior was stronger than for the blends, whereas pure HPMC showed the lowest viscosity and the least shear-thinning behavior. Regarding this, at low temperatures, HPMC was a sol, of which the

viscosity was much lower than that of HPS. The addition of HPMC decreased the shear-thinning behavior of HPS. Besides, with a higher MS of HPS, the viscosity of the HPMC/HPS solution at a fixed blend ratio displayed a reduced viscosity. This can be explained by the reduced intermolecular hydrogen bonding because of hydroxypropylation. In the low-shear stage, there was a stable-value region in the samples containing HPS with a high MS, and the stable-value region was narrowed with the addition of HPMC.

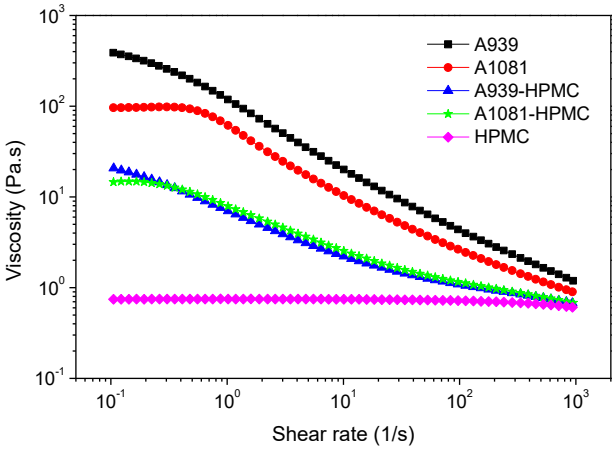

Fig. 1. Viscosity vs. shear rate curves for the solutions of HPMC, HPSs with different MSs, and HPMC/HPS blends with the different HPSs at 25 °C (with pre-shearing)

Table 1 lists the *n* (flow behavior index) and *K* (fluid consistency index) values for the different samples calculated in the shear rate range of 10^{-1}–10^{3} 1/s. For all the samples, *n* was less than 1, indicating that they are all pseudoplastic fluids. With a higher HPMC content, HPMC/HPS blends displayed a higher *n* value, suggesting an enhanced Newtonian behavior. However, *K* (proportional to viscosity) was decreased with a higher amount of HPMC. For pure HPS, both *n* and *K* were decreased with a higher MS of HPS, meaning hydroxypropylation can improve the pseudoplasticity and reduce the viscosity of the starch solution. For the blend samples, *n* was close to 1 and decreased

with the increased MS of HPS, which shows the effect of starch hydroxypropylation on the overall rheological behavior of the blends.

According to blending principle, the smaller the difference in viscosity between two phases, the greater is the compatibility between two components (Larson, 1999). HPMC showed a Newton-like liquid (*n* close to 1) at low temperatures. Therefore, in this study, a higher *n* value of HPS suggests better compatibility in the blends.

3.1.2 Dynamic rheological properties

3.1.2.1 Linear viscoelastic regions

It is well known that for a hydrogel, G' is controlled by the hardness, junction zone strength, and bonds quantities of effective molecular chains. In addition, G'' is contributed by the friction energy consumption in a liquid state, which involves the mobility, movement and friction of small molecules, and the vibration and rotation of functional groups. The crossover of G' and G'' ($\tan \delta = 1$) indicates the sol-gel transition. G' and G'' can be used to detect the gelation behavior, the speed of gel network formation, and structural characteristics (Clark and Ross-Murphy, 1987). They also reflect the inner structural development and molecular interactions during the gel network formation (Musampa et al., 2007).

Fig. 2 shows the results from strain sweep measurements performed over a strain range of 0.01–100% at a frequency of 1 Hz. It can be seen that at low strains (0.01–1%), all the samples except HPMC were gel ($G' > G''$). For HPMC, G' was always lower than G'' in the test range, indicating HPMC was a solution. Besides, different samples had viscoelasticity that had different degrees of dependence on strain. For G80, this dependence was more apparent — when the strain was higher than 0.3%, there was an apparent decrease in G', a remarkable increase in G'', and a dramatic

increase in tan δ. Moreover, a crossover of G' and G'' was observed for G80 at a strain of 1.7%. This means that G80 became a solution when the strain was over 1.7%.

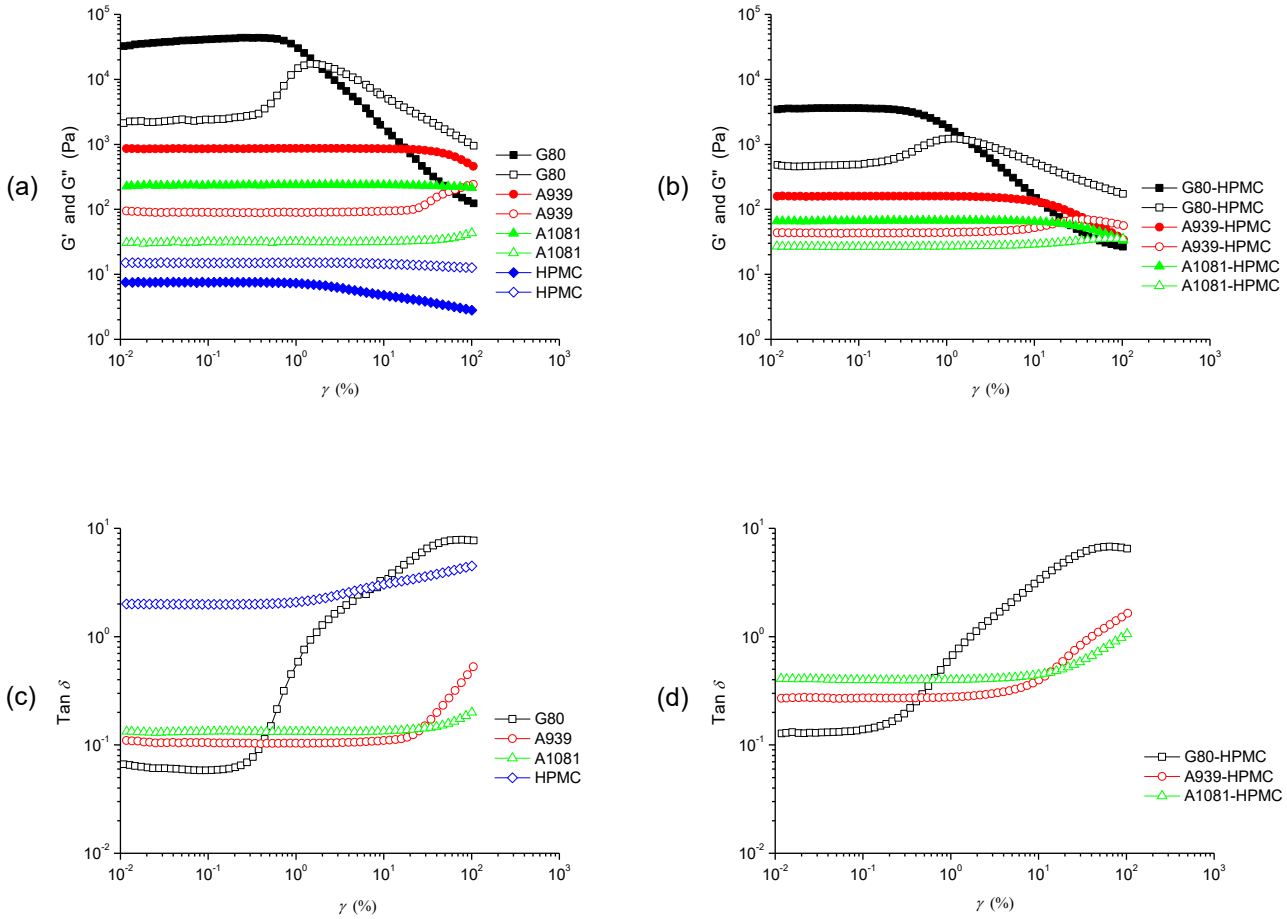

Fig. 2. Strain sweep curves for the solutions of HPMC, HPSs with different MSs, and HPMC/HPS blends with the different HPSs at a frequency of 1 Hz at 25 °C. In (a) and (b), the solid and hollow symbols represent G' and G'', respectively.

For HPS, the linear viscoelastic region was narrowed with a lower MS. In other words, with the increased MS, the sudden change in tan δ occurred at a higher strain. G80 had the smallest

viscoelastic range among all the samples. This value was taken into consideration for the choice of strain in the following studies.

For HPMC/HPS blends, the linear viscoelastic region was also narrowed with a lower MS, although this MS-induced narrowing of the linear viscoelastic region became less apparent.

3.1.2.2 Viscoelastic property during heating and cooling

Fig. 3 shows the dynamic viscoelastic properties of HPMC, HPS samples with different MSs, and HPMC/HPS blends with different HPSs. It can be seen that for HPMC, there were four regions during heating, namely a plateau, two structural formation stages, and then another plateau. During the first plateau, G' was below G'' and both of them were very small and decreased slowly with increasing temperature. This indicates a common viscoelastic behavior of a liquid. The thermal gelation of HPMC had two distinct stages of the structural formation and the divide was the crossover of G' and G'' (*i.e.*, the sol-gel transition at *ca.* 49 °C), which was consistent with other reports (Haque and Morris, 1993; Haque et al., 1993). At higher temperatures, due to the association of hydrophobic groups and that of hydroxyl groups, a crosslinked network was gradually formed (Chen, 2007; Dziesak, 1991; Schmitz et al., 2006). The last plateau with higher G' and G'' indicates the eventual formation of a gel network.

HPMC

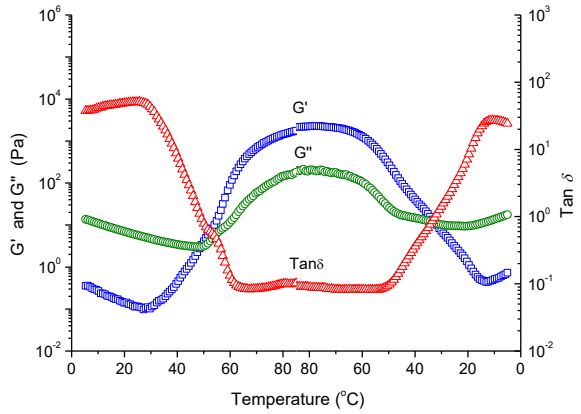

282

G80

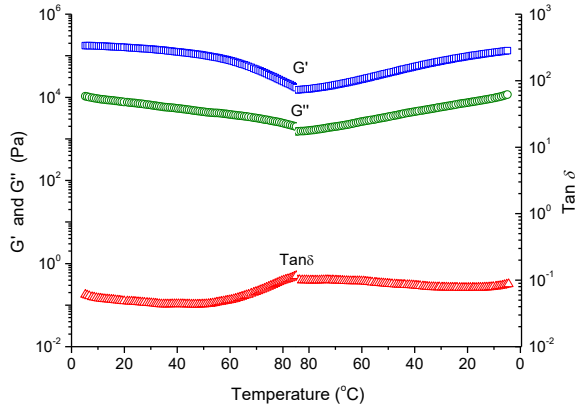

G80-HPMC

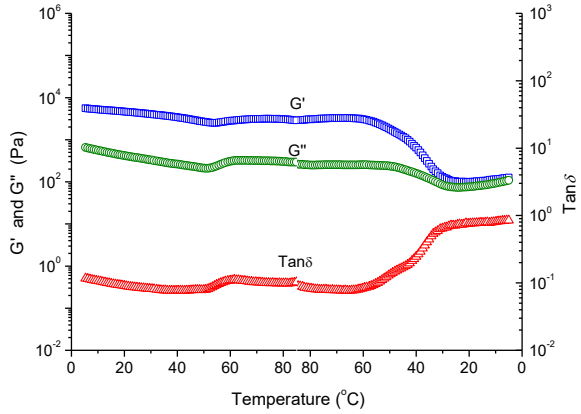

283

A939

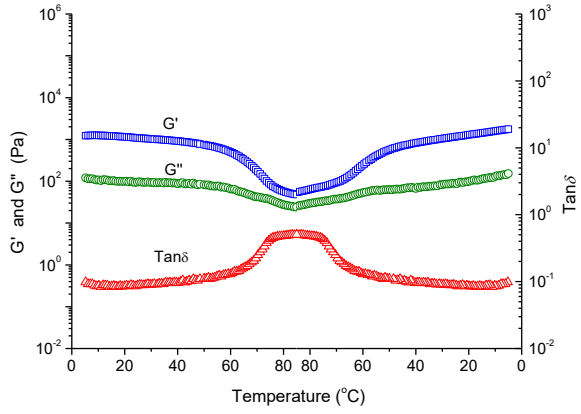

A939-HPMC

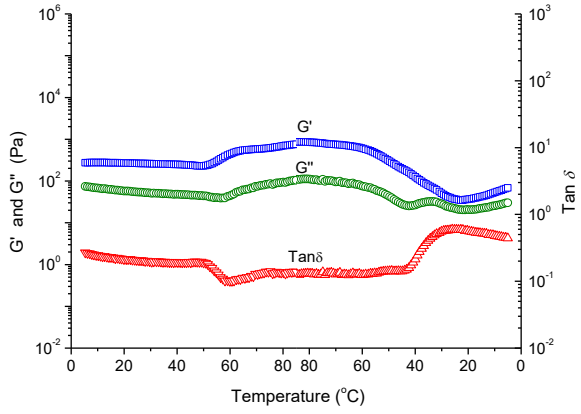

284

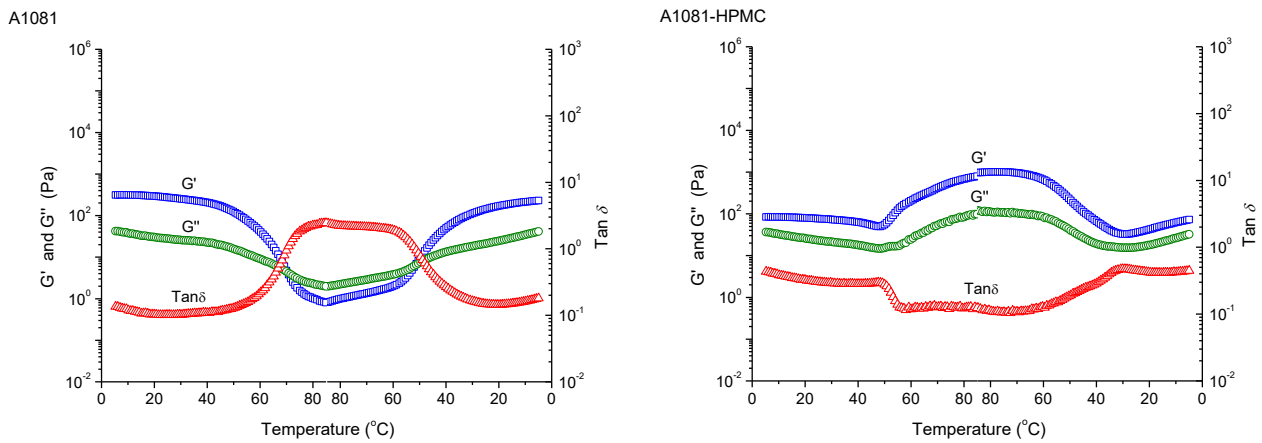

285

286 **Fig. 3.** Storage modulus (*G′*), loss modulus (*G″*) and tan *δ vs.* temperature curves for the solutions of
287 HPMC, HPSs with different MSs, and HPMC/HPS blends with the different HPSs.

288

289

290 With decreasing temperature, the sequence of these regions was reversed. The crossover of *G′*
291 and *G″* shifted to a lower temperature of about 32 °C during cooling. This shift could be due to
292 hysteresis (Haque and Morris, 1993) and/or the condensation of chains at a lower temperature (Chen,
293 2007; Zhang et al., 2015). Like HPMC, most of the other samples displayed these four regions
294 during heating, which were reversed during cooling. However, we can see that G80 and A939
295 showed a simpler pattern with no crossover of *G′* and *G″*. G80 even did not reach any plateau finally.
296 For HPS, a higher MS could shift both the starting and end temperatures for the structural
297 formation (gelation). Specifically, the starting temperatures of G80, A939 and A1081 were 61 °C,
298 62 °C and 54 °C, respectively. Besides, the higher the MS, the lower were both *G′* and *G″*, which
299 was in agreement with other studies (Kim et al., 1992a; Kim et al., 1992b). This suggests that the gel
300 texture became softer with the increased MS. Regarding this, the ordered structure of starch was
301 disrupted, and its hydrophilicity was increased when native starch was hydroxypropylated
302 (Morikawa and Nishinari, 2000).

For all the blends, both G' and G'' were decreased with a higher MS of HPS, which was consistent with results for pure starches. Also, the effect of MS on both G' and G'' for the blends became less apparent with the addition of HPMC.

All the blend samples showed a similar pattern of viscoelastic properties, which was parallel to those for HPS at low temperatures and HPMC at high temperatures. In other words, HPS controlled the viscoelastic property of the blends at low temperatures whereas HPMC dominated the behavior at high temperatures. These results might be accounted for by the different gelation properties of HPS and HPMC. Specifically, HPS is a cooling gel, shifting from gel to sol during heating. In contrast, HPMC, as a thermal gel, congeals with increasing temperature. For HPMC/HPS blends, at low temperatures, HPS mainly contributed to the gelation, while at high temperatures, HPMC was responsible for the gel formation.

The blends had intermediate moduli between those for individual HPS and HPMC. Besides, G' was always higher than G'' during the whole temperature range. In this regards, both HPS and HPMC could individually form intermolecular hydrogen bonding with water and with each other. Furthermore, all the blends showed a tan δ peak at about 45 °C, suggesting a change of the continuous phase in the matrix.

3.1.2.3 Dynamic mechanical properties

Fig. 4a and b show the moduli (G' and G'') *vs.* frequency results at 5 °C for HPMC, HPSs with different MSs, and HPMC/HPS blends with different HPSs. All the HPS samples showed a typical solid-like behavior ($G' > G''$), whereas HPMC was fluid-like ($G' < G''$). All the blends had a solid-like behavior. For most of the samples, a higher frequency led to higher G' than G'', indicating the materials were more solid-like.

328

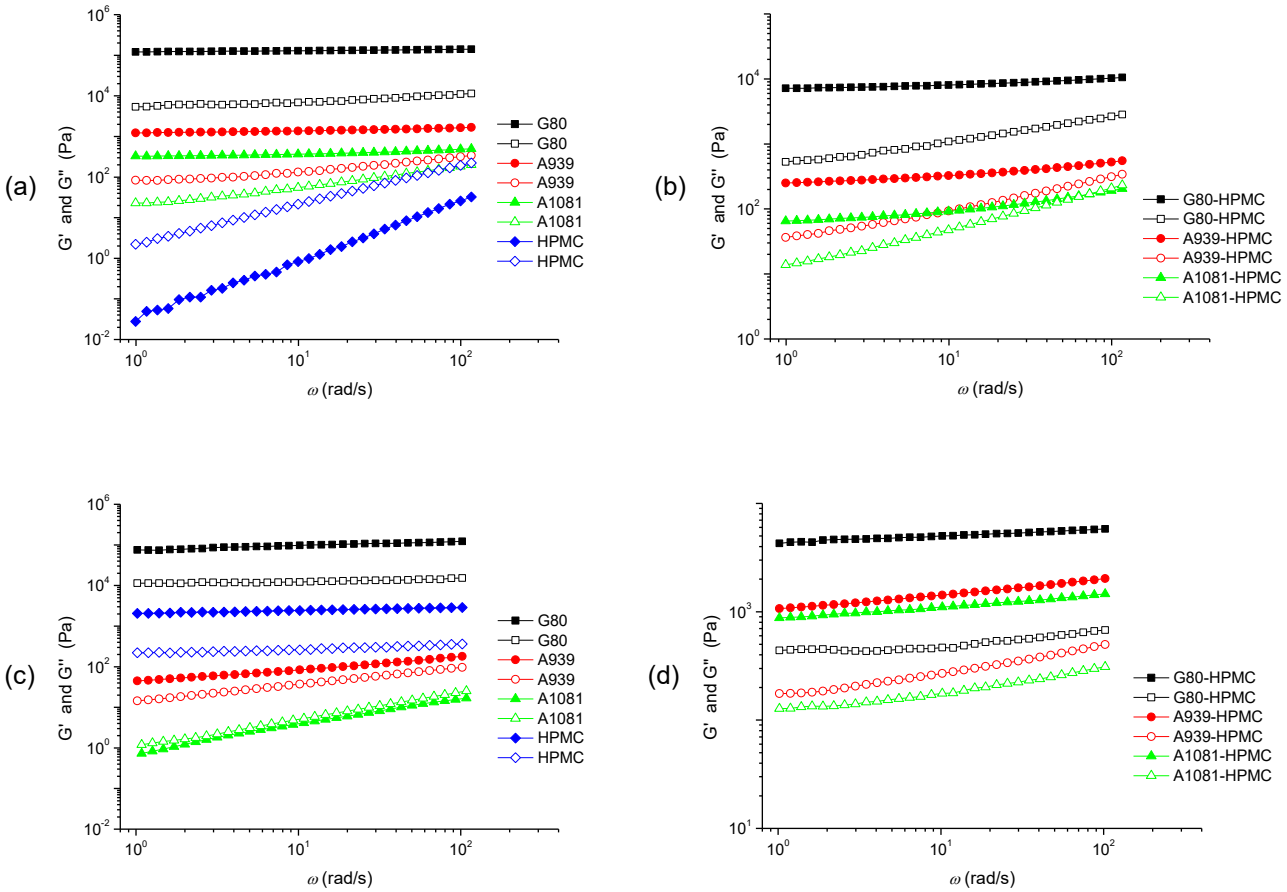

329

330 **Fig. 4.** Storage modulus (G') and loss modulus (G'') *vs.* frequency curves for HPMC, HPSs with
331 different MSs, and HPS/HPMC blends with the different HPSs at 5 °C (a and b) and 85 °C (c and d).
332 The closed and open symbols correspond to G' and G'', respectively.

333

334

335 **Table 2** lists the n', n'', G_0' and G_0'' values for different samples at 5 °C. For all the HPS samples,
336 n' was close to 0, and G_0' was much higher than G_0'', confirming their solid- like behavior (Ortega-
337 Ojeda et al., 2004). HPMC showed clearly a fluid-like behavior since the slopes were close to 1. For
338 the blends, n' and n'' were slightly higher than those for HPSs, suggesting that the blends behaved
339 less like a solid than HPSs.

340 HPMC showed an apparent frequency-dependence, whereas such a dependence could hardly be
341 observed for HPSs. The blends showed some degree of dependence on frequency. For all the

samples containing HPS, n' was much lower than n'', and G'' was more dependent on frequency than G', suggesting that these samples were more elastic and less viscous (Clark and Ross-Murphy, 1987; Park et al., 2004; Rosalina and Bhattacharya, 2002). Therefore, the properties of the blends were mainly contributed by HPS. This was especially true considering HPMC was a liquid with a lower viscosity at a lower temperature.

Both n' and n'' for HPS were increased with a higher MS, indicating that hydroxypropylation reduced the solid-like behavior of the starch and increased the frequency-dependence at low temperatures. This trend regarding the effect of hydroxypropylation was also evident in the blend samples. For both HPSs and the blends, G_0' and G_0'' were also decreased with the increased MS of HPS, which may be attributed to the weakened viscoelasticity of HPS as the main contributing component.

Fig. 4c and d show the moduli (G' and G'') *vs.* frequency results for HPSs with different MS, HPMC, and HPMC/HPS blends with different HPSs at 85 °C. All HPSs, except A1081, showed typical solid-like behavior. For A1081, G' was very close to but lower than G'', indicating a fluid-like behavior. This might be ascribed to the gel-sol transition of A1081 as a cooling gel at a high temperature. On the other hand, an increased MS could decrease n', n'', G_0' and G_0'' (**Table 2**), indicating that hydroxypropylation made the starch behave less like a solid at 85 °C. Specifically, for G80, both n' and n'' were close to 0, indicating its solid-like behavior. In contrast, for A1081, n' and n'' were close to 1, showing its fluid-like behavior. These results of n' and n'' were also in accordance with the G' and G'' data. Furthermore, it can be seen in **Fig. 4c and d** that a higher MS significantly increased the frequency-dependence of HPS.

Fig. 4c and d show that at 85 °C, HPMC had a typical solid-like behavior ($G'>G''$), which could be ascribed to its thermal-gelation property. In addition, for HPMC both G' and G'' were not apparently varied, indicating their negligible frequency-dependence.

For all the blends, both n' and n'' were close to 0, and G_0' was much higher than G_0'' (**Table 2**), confirming their solid-like behavior at 85 °C. On the other hand, while a higher MS could change the behavior of HPS from being solid-like to liquid-like (as discussed above), this phenomenon was not observed in the blends. Besides, for the blends containing HPMC, both G' and G'' remained stable with increased frequency. Moreover, for all the blends, n' and n'' were close to those for HPMC. All these results suggest that it was HPMC that mainly contributed to the properties of the blend gels at a high temperature (85 °C).

3.1.3 Thixotropic property

Fig. 5 shows a three-interval thixotropic behavior of the HPMC/HPS blend solutions with different MSs of HPS. All the samples were thixotropic since the viscosity of the third stage (the structural recovery stage) was lower than that of the first stage. At the low-shear stage (the first stage), the solution viscosity was decreased with the increased content of HPMC and a higher MS of HPS. These are consistent with the results of steady rheological properties.

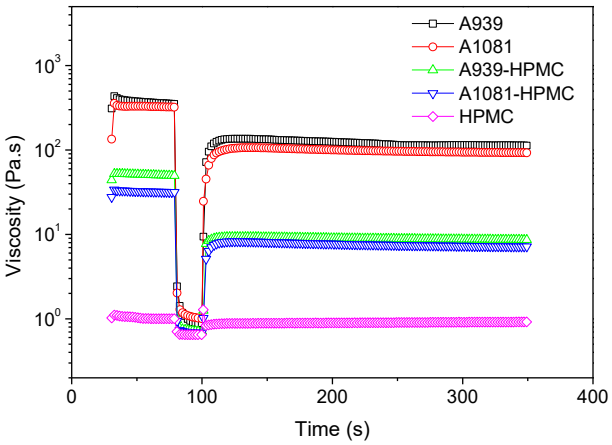

Fig. 5. Three-interval thixotropic curves for the solution of HPMC, HPSs with different MSs, and HPMC/HPS blends with the different HPSs at 5 °C.

The structural recovery data of three-interval thixotropic tests were listed in **Table 2**. A higher structural recovery ratio (DSR) led to a weakened thixotropic behavior. The DSR values of pure HPSs were obviously lower than that of pure HPMC in the same structural recovery time. Regarding this, HPMC molecular chains were rigid with a short relaxation time, which means the structure could recover within a short time. In contrast, HPS molecular chains were flexible and the relaxation time was relatively long, thus the structural recovery of HPS was slow. For pure HPS, the DSR was decreased with a higher MS, indicating that hydroxypropylation improved the flexibility of starch molecular chains and prolonged the relaxation time of HPS. For the blend samples, the DSR values were lower than those of pure ones, and increased with a higher MS of HPS. This result suggests that the thixotropic behavior of the blends was weakened with the increased MS of HPS.

3.2 Characteristics of films

3.2.1 Crystalline structure

Fig. 6 shows the SAXS patterns of HPMC/HPS blend films. All the samples present apparent characteristic peaks in a relatively larger scale range (q > 0.3 Å^{-1}). From **Fig. 6a**, HPMC showed a well-defined peak at about 0.569 Å^{-1}, corresponding to its crystalline structure at 7.7°. In contrast, HPSs showed a well-defined peak at about 0.397 Å^{-1}, corresponding to the typical B-type crystalline structure of starch at 5.3°. Besides, the characteristic peak area of A939 was higher than that of A1081, suggesting that a higher MS led to a decreased characteristic peak area. Regarding this, the incorporation of hydroxypropyl groups in the starch molecules may destroy the original crystalline structure of starch, and make it less easy for intermolecular rearrangement and crosslinking, which inhibit the recrystallization of starch.

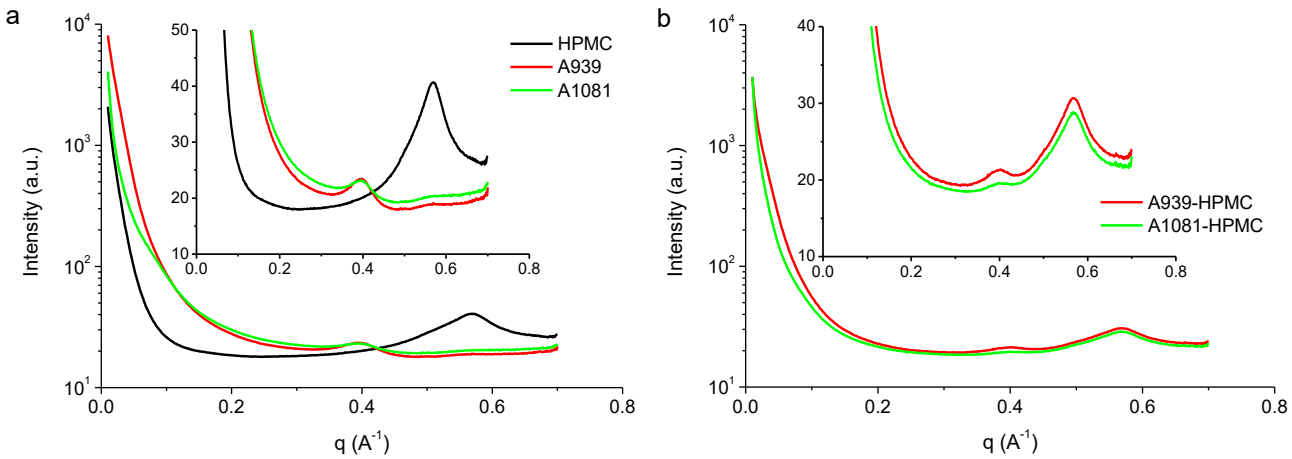

Fig. 6. SAXS patterns for the films of HPMC, HPSs with different MSs, and HPMC/HPS blends with the different HPSs.

Fig. 6b shows the SAXS patterns of the blend films. All the blend samples showed two SAXS peaks at about 0.569 $Å^{-1}$ and 0.397 $Å^{-1}$, corresponding to the characteristic peak of HPMC (at 7.7°) and HPS (at 5.3°), respectively. The HPS characteristic peak area of HPMC/A939 was larger than that of HPMC/A1081, attributed to the inhibition of orderly rearrangement between starch molecules due to the increase of hydroxypropylation. This relationship between the peak area and the MS of HPS corresponds to that in pure HPS. On the other hand, the area of the characteristic peak of HPMC at 7.7° did not show apparent changes with the variation in MS. Moreover, compared with the corresponding pure samples, both the HPMC and HPS characteristic peak areas for the blends were smaller. This observation indicates that both HPMC and HPS could inhibit the recrystallization of the other component to a certain degree in the blends.

3.2.2 Fractal structure

Fractal geometry has been used as a natural description for disordered objects possessing dilation symmetry, meaning that they look geometrically self-similar under transformation of scale such as changing the magnification of a microscope. The fractal dimension (D) can be calculated according to the Porod equation:

$$I(q) \propto q^{-\alpha} \qquad (5)$$

where I is the SAXS intensity and α is an exponent called the Porod slope. The relation between α and D follows $D_m = \alpha$ ($\alpha < 3$) representing a mass fractal, or $D_s = 6 - \alpha$ ($3 < \alpha < 4$) indicating a surface fractal. D_m is used to indicate the compactness while D_s can be regarded as an indicator of the degree of smoothness (Zhang et al., 2013a). For polysaccharides such as starch and cellulose, the average chain length is between 1000 and 1500 nm. If this value is called R, we have $q_R >> 1$. In our

work, the Porod slopes α of all samples are below 3 and thereby $D_m = \alpha$, which we called D in the following text.

Fig. 7 shows the ln$I(q)$–ln$q$ patterns and its fit curves for HPMC/HPS blend films. All the samples were seen to have a self-similar fractal structure within a certain limit. All the Porod slopes were smaller than 3, indicating HPMC/HPS films had a smooth surface. The fractal structure parameters of HPMC/HPS blend films were provided in **Table 3**. When pure HPS was concerned, the D value of A939 was higher than that of A1081, suggesting the density of the self-similar structure in the films decreased with a higher MS. Regarding this, the incorporation of hydroxypropyl groups in starch molecules prevented the association of HPS chains and led to a self-similar structure with a lower density. The hydrophilic hydroxypropyl groups could form intermolecular hydrogen bonding with water, thus the interaction between HPS chains was lessened. The bulky hydroxypropyl groups could also limit the reassociation and crosslinking of starch molecular chains. Therefore, the self-similar structure of HPS films became looser with the increased MS of HPS.

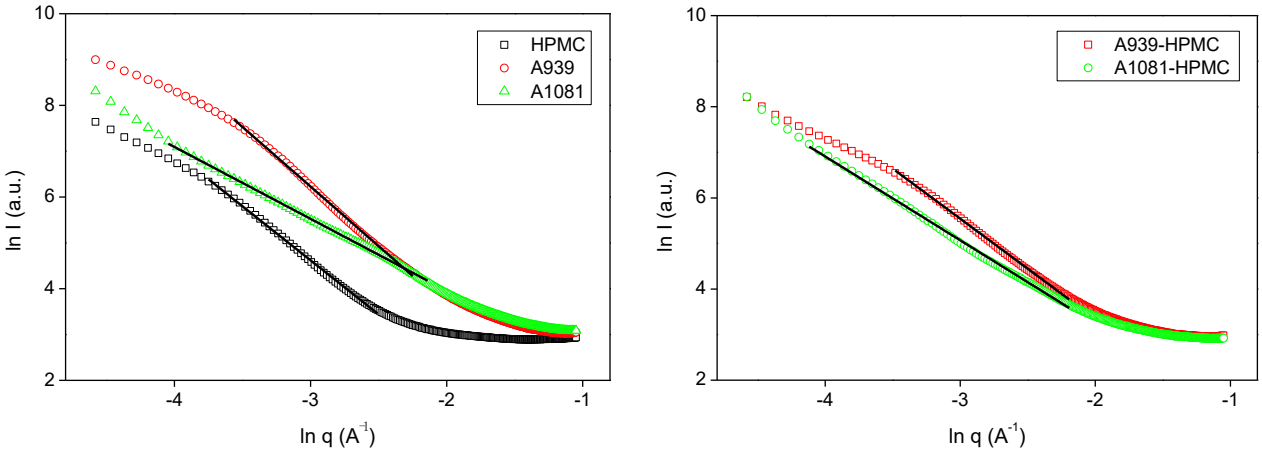

Fig. 7. ln$I(q)$–ln$q$ patterns and their fit curves for the films of HPMC, HPSs with different MSs, and HPMC/HPS blends with the different HPSs.

The *D* value of pure A939 was higher than that of pure HPMC. This higher *D* value of pure A939 could be attributed to the starch recrystallization, the more ordered structure between starch molecular chains, and a self-similar structure with a higher density that were formed in its films. The *D* value of the HPMC/A939 blend was the lower than either pure A939 or pure HPMC, as blending could hamper the chain association of individual components and reduce the density of the self-similar structure of the starch.

In contrast, for HPMC/A1081, the *D* value of A1081 was lower than that of HPMC. This might be due to the inhibition of the starch retrogradation with the incorporation of hydroxypropyl groups, thus the self-similar structure in the film became looser. The *D* value of the HPMC/A1081 blend was higher than that of pure A1081, which is different from the case of the HPMC/A939 system. Regarding this, the HPS with a high MS could possibly form a self-similar structure with larger cavities, and the linear HPMC molecules could enter the cavities resulting in a higher density of the self-similar structure. This also implies that a more homogeneous compound could be formed by HPMC and HPS with a high MS. In agreement with this, the rheological results have shown that

475 hydroxypropylation could reduce the viscosity of starch and the viscosity difference between the two
476 components in the blends, which is favorable for forming more homogeneous blends.
477

478 ### 3.2.3 Tensile properties

479 The E, σ_t and ε_b of HPMC/HPS films were listed in **Table 4**. For pure HPS films, a higher MS of
480 HPS led to lower E and σ_t and higher ε_b, indicating that hydroxypropylation reduced the film rigidity
481 and improved the flexibility. Given this, the hydroxypropyl groups might have resulted in a looser
482 film structure (as confirmed by the fractal structure results) and inhibited the starch retrogradation (as
483 shown by the crystallinity analysis).
484 For the blend films, increasing the MS of HPS led to decreased E and increased σ_t and ε_b. The
485 change in the MS of HPS could vary not only the properties (viscosity and mechanical properties) of
486 HPS itself but also the compatibility between the two polymers. A higher MS could result in a lower
487 viscosity of the HPS, which could improve the compatibility between HPS and HPMC. On the other
488 hand, for HPMC/A1081 blends, with the increased content of the starch, E and σ_t were decreased,
489 whereas ε_b was increased apparently. This result is in agreement with a previous study (Wang et al.,
490 2016a) and suggests that a higher degree of hydroxypropylation may decrease the intermolecular
491 interactions and thus the mechanical properties.
492

493 ### 3.2.4 Oxygen permeability

494 Edible films with a good oxygen barrier property can help to improve food quality and extend
495 food shelf life since that the oxidation caused by oxygen is an initial stage of several forms of food
496 deterioration (Klangmuang and Sothornvit, 2016). Thus, we studied the oxygen permeability (OP) of
497 HPMC/HPS films with the varied MS of HPS and the results are provided in **Table 5**. It is seen that
498 the OP values of pure HPS films were all much lower than that of the pure HPMC film, confirming

the better oxygen barrier property of starch films (Ortega-Toro et al., 2014; Wang et al., 2016a). For pure HPS films, the content of hydroxypropyl groups had a significant effect on the oxygen barrier property. The OP of A1081 (0.64) was almost six times that of A939 (0.11). The OP increased with a higher MS of HPS. Regarding this, as confirmed by the fractal structure results, the incorporation of hydroxypropyl groups declined the density of films, which could enlarge the permeability channel for oxygen in the film.

For the blend films, the OP was decreased with a higher MS of HPS, which is opposite to the case of pure HPS. In the HPMC/HPS (5:5) blend, the HPS with a higher viscosity was dispersed in the continuous phase of HPMC with a lower viscosity. Again, the viscosity of the HPS decreased with a higher MS, and leading to better compatibility between the two polymers. There could be competing effects of hydroxypropylation on expanding the oxygen permeation area and of blending on enhancing the tortuosity of oxygen permeation channel. With a better compatibility, the latter effect outperformed the former, leading to the decreased OP of the blend films.

3.2.5 Thermal degradation

Fig. 8 shows the TGA results of the pure HPMC film, pure HPS films, and HPS/HPMC blend films. For all the films, there were two thermal degradation stages, namely the moisture evaporation from the materials in the temperature range of 30–180 °C and the thermal decomposition of polysaccharides in the temperature range of 300–400 °C. Pure HPS films displayed a similar peak at 310 °C (A939) and 305 °C (A1081), respectively. The pure HPMC film showed a higher thermal stability, with its decomposition occurring at 365 °C. All the blend samples showed two decomposition peak representing HPS and HPMC respectively. However, for the blends, the HPS thermal decomposition occurred at a reduced temperature while the HPMC peak temperature was not apparently affected. Thus, blending reduced the thermal stability of the HPS component, which

might be due to the interaction of HPMC with HPS and thus the further reduced intermolecular interactions between HPS molecular chains and the reduced ordered structure in HPS.

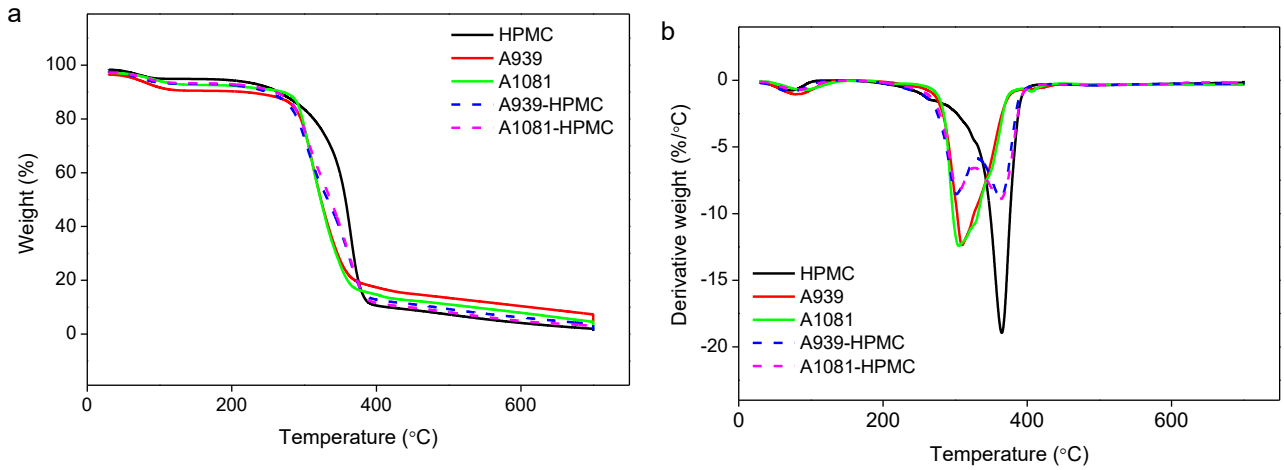

Fig. 8. TGA curves (a) and their derivative curves (b) of the films of HPMC, HPSs with different MSs, and HPMC/HPS blends with the different HPSs.

3.2.6 Relationship between rheological properties, structure, and film performance

For the blends, the compatibility between and the physicochemical properties of the constituents exert varying levels of influence on rheology (Chhabra and Richardson, 2008). However, the rheological history and structure ultimately determine the performance of the products. For each product, there is a degree of its own complexity and peculiarities, which need to be incorporated into the structure-rheology link.

Basing on the rheology results, it is noticeable that the rheological properties showed an obvious dependence on the MS of HPS. For pure HPS, a higher MS caused a lower viscosity and an enhanced Newtonian-behavior, which reduced the different in viscosity between the two components and thus induced a greater compatibility in the blends. The thixotropic property was increased with a higher MS, attributed to the improved flexibility of starch chains by hydroxypropylation. Such changes

resulted in a much more flexible texture of the films, which conformed to the change in E and σ_t in the tensile properties. The SAXS results clearly show that the fractal dimension (D) was strongly depended on the MS of HPS. For pure HPS, a higher MS caused greater compactness of the self-similar structure. Such changes induced larger permeable channels for oxygen in the films and the reduced rigidity of the films, which correspond to the changes in oxygen permeability, E and σ_t. The WAXS results clearly suggest that the crystalline structure strongly depended on the MS of HPS. A higher MS caused a decreased characteristic peak area. This change was due to the inhibition of starch recrystallization, and induced a much higher ε_b value.

The changes in the structure and rheological properties certainly affected the blend film performance. The SAXS data show that a good compatibility between the two components caused a much denser structure and better tensile properties of the films. Therefore, the film performance of the blends could be largely affected by the changes in MS and the compatibility between the two components. A higher MS caused larger permeable channels for oxygen in the films. Besides, an increased MS also led to a better compatibility between two components, which resulted in increased tortuosity of the oxygen permeation channels. The final OP of blends was determined by these two competing factors. Regarding the tensile properties, both a higher MS of HPS and a better compatibility induced higher ε_b; therefore, the ε_b value of the blends was increased with a higher MS. The thixotropic behavior was also balanced by the MS of HPS and the storage modulus of the gel. With a higher MS, the thixotropic property was declined due to the decreased storage modulus of HPS. At a low temperature, HPS was the dispersion phase with a high viscosity, which was confirmed by the changes in viscoelastic properties during heating and cooling. The competition between these two aspects could reduce the influence of MS on the thixotropic behavior.

4 Conclusion

This work concerns the effect of hydroxypropylation of starch on the rheological properties and the film structure and performance of a novel thermal/cooling-gel bi-phasic system. This system was based on two natural biopolymer-based hydrogels, HPMC and HPS, which could form continuous phases at low and high temperatures, respectively. The variation of this phase conformation significantly influenced the rheological properties, thixotropy, and gel properties of the blend systems, and subsequently affected the crystalline structure, fractal structure, mechanical properties, OP, and thermal stability of the blend films. In particular, HPS at low temperatures, and HPMC at high temperatures, play a dominant role in controlling these different properties.

The rheological and gel properties were also significantly affected by the starch chemical modification. A higher MS of HPS decreased the viscosity and weakened the shear thinning behavior of the blend solutions at low temperatures and also declined the G' and G'' of the hybrid gels. Regarding this, the hydroxypropylation of native starch could break the intermolecular hydrogen bonding, disrupt its ordered structure, increase its hydrophilicity, and result in a softer gel texture. A higher MS could also increase n' and n'', indicating that hydroxypropylation reduced the solid-like behavior and increased the frequency-dependence. However, blending HPS with HPMC made these effects of the MS of HPS on the rheological and gel properties less apparent. On the other hand, the film structure and performance was also significantly affected by the starch hydroxypropylation. With a higher MS of HPS, the starch crystallinity was decreased and the elongation at break of films was increased, indicating the hydroxypropylation of starch could inhibit the molecular rearrangement and improve the flexibility of films. However, an increase in the MS of HPS also led to reduced fractal structure and OP. This suggests that a higher film density could be linked to a better oxygen barrier property.

Our results here have shown that the processability and performance of HPMC/HPS biphasic systems could be improved by the chemical modification of starch. With the versatile chemistry of

590 starch and cellulose, new materials based on this kind of systems could be developed to suit the
591 needs of high-value applications such as biomedical materials, food, and coatings.
592

593 Acknowledgements

594 This work was financially supported by the National Natural Science Foundation of China
595 (NSFC) (Nos. 31130042 and 31571789) and the Special Funds for Taishan Scholars Projects of
596 Shandong Province. Y. Wang would like to acknowledge the China Scholarship Council (CSC) for
597 providing financial assistance for her visiting studies at the CSIRO in Australia. F. Xie acknowledges
598 the European Union's Marie Skłodowska-Curie Actions (MSCA) and the Institute of Advanced
599 Study (IAS), University of Warwick for the Warwick Interdisciplinary Research Leadership
600 Programme (WIRL-COFUND). Part of this research was undertaken on the SAXS/WAXS beamline
601 at the Australian Synchrotron, Victoria, Australia.
602

603 References

604 Adak, S., Banerjee, R., 2016. A green approach for starch modification: Esterification by lipase and novel
605 imidazolium surfactant. Carbohyd. Polym. 150, 359-368.
606 Chen, H.H., 2007. Rheological properties of HPMC enhanced Surimi analyzed by small- and large-strain
607 tests: I. The effect of concentration and temperature on HPMC flow properties. Food Hydrocolloid. 21, 1201-
608 1208.
609 Chhabra, R.P., Richardson, J.F., 2008. Non-Newtonian Fluid Behaviour, in: Richardson, J.F. (Ed.), Non-
610 Newtonian Flow and Applied Rheology：Engineering Applications. Elsevier Ltd, pp. 1-55.
611 Chun, S.Y., Yoo, B., 2007. Effect of molar substitution on rheological properties of hydroxypropylated rice
612 starch pastes. Starch-Starke. 59, 334-341.

613 Clark, A.H., Ross-Murphy, S.B., 1987. Structural and Mechanical Properties of Biopolymer Gels, in: Abe, A.,
614 Dusek, K., Kobayashi, S. (Eds.), Biopolymers. Springer, Berlin Heidelberg, pp. 57-192.
615 Correa, M.J., Anon, M.C., Perez, G.T., Ferrero, C., 2010. Effect of modified celluloses on dough rheology and
616 microstructure. Food Res. Int. 43, 780-787.
617 Cuq, B., Gontard, N., Guilbert, S., 1998. Proteins as agricultural polymers for packaging production. Cereal.
618 Chem. 75, 1-9.
619 Dhillon, S., Seetharaman, K., 2011. Rheology and texture of starch gels containing iodine. J. Cereal Sci. 54,
620 374-379.
621 Dziesak, J.D., 1991. A focus on gums. Food Technol.-Chicago. 45, 118-132.
622 Han, J.A., Lee, B.H., Lim, W.J., Lim, S.T., 2005. Utilization of hydroxypropylated waxy rice and corn
623 starches in Korean waxy rice cake to retard retrogradation. Cereal. Chem. 82, 88-92.
624 Haque, A., Morris, E.R., 1993. Thermogelation of methylcellulose .1. Molecular-structures and processes.
625 Carbohyd. Polym. 22, 161-173.
626 Haque, A., Richardson, R.K., Morris, E.R., Gidley, M.J., Caswell, D.C., 1993. Thermogelation of
627 methylcellulose .2. Effect of hydroxypropyl substituents. Carbohyd. Polym. 22, 175-186.
628 Heyman, B., De Vos, W.H., Depypere, F., Van der Meeren, P., Dewettinck, K., 2014. Guar and xanthan gum
629 differentially affect shear induced breakdown of native waxy maize starch. Food Hydrocolloid. 35, 546-556.
630 Imran, M., Klouj, A., Revol-Junelles, A.M., Desobry, S., 2014. Controlled release of nisin from HPMC,
631 sodium caseinate, poly-lactic acid and chitosan for active packaging applications. J. Food. Eng. 143, 178-185.
632 Kadokawa, J.I., Murakami, M.A., Takegawa, A., Kaneko, Y., 2009. Preparation of cellulose-starch composite
633 gel and fibrous material from a mixture of the polysaccharides in ionic liquid. Carbohyd. Polym. 75, 180-183.
634 Kaur, L., Singh, N., Singh, J., 2004. Factors influencing the properties of hydroxypropylated potato starches.
635 Carbohyd. Polym. 55, 211-223.
636 Kim, H.R., Eliasson, A.C., Larsson, K., 1992a. Dynamic rheological studies on an interaction between lipid
637 and various native and hydroxypropyl potato starches. Carbohyd. Polym. 19, 211-218.
638 Kim, H.R., Hermansson, A.M., Eriksson, C.E., 1992b. Structural characteristics of hydroxypropyl potato
639 starch granules depending on their molar substitution. Starch-Starke. 44, 111-116.

640 Klangmuang, P., Sothornvit, R., 2016. Barrier properties, mechanical properties and antimicrobial activity of
641 hydroxypropyl methylcellulose-based nanocomposite films incorporated with Thai essential oils. Food
642 Hydrocolloid. 61, 609-616.
643 Larson, R.G., 1999. Foams, Emulsions, and Blends, in: Larson, R.G. (Ed.), The Structure and Rheology of
644 Complex Fluids. Oxford University Press, New York, pp. 388-437.
645 Lawal, O.S., Ogundiran, O.O., Adesogan, E.K., Ogunsanwo, B.M., Sosanwo, O.A., 2008. Effect of
646 hydroxypropylation on the properties of white yam (Dioscorea rotundata) starch. Starch-Starke. 60, 340-348.
647 Lee, H.L., Yoo, B., 2011. Effect of hydroxypropylation on physical and rheological properties of sweet potato
648 starch. LWT-Food Sci. Technol. 44, 765-770.
649 Li, L., 2002. Thermal gelation of methylcellulose in water: Scaling and thermoreversibility. Macromolecules.
650 35, 5990-5998.
651 Liu, H., Yu, L., Xie, F., Chen, L., 2006. Gelatinization of cornstarch with different amylose/amylopectin
652 content. Carbohyd. Polym. 65, 357-363.
653 Liu, S.Q., Joshi, S.C., Lam, Y.C., Tam, K.C., 2008. Thermoreversible gelation of
654 hydroxypropylmethylcellulose in simulated body fluids. Carbohyd. Polym. 72, 133-143.
655 Luallen, T., 2004. Utilizing starches in product development, in: Eliasson, A.C. (Ed.), Starch in Food:
656 Structure, Function and Applications. Woodhead Publishing, New York, pp. 393-424.
657 Masina, N., Choonara, Y.E., Kumar, P., du Toit, L.C., Govender, M., Indermun, S., Pillay, V., 2017. A review
658 of the chemical modification techniques of starch. Carbohydr Polym. 157, 1226-1236.
659 Moin, A., Ali, T.M., Hasnain, A., 2017. Characterization and utilization of hydroxypropylated rice starches
660 for improving textural and storage properties of rice puddings. International Journal of Biological
661 Macromolecules. 105, 843-851.
662 Morikawa, K., Nishinari, K., 2000. Rheological and DSC studies of gelatinization of chemically modified
663 starch heated at various temperatures. Carbohyd. Polym. 43, 241-247.
664 Musampa, R.M., Alves, M.M., Maia, J.M., 2007. Phase separation, rheology and microstructure of pea
665 protein-kappa-carrageenan mixtures. Food Hydrocolloid. 21, 92-99.
666 Ortega-Ojeda, F.E., Larsson, H., Eliasson, A.C., 2004. Gel formation in mixtures of amylose and high
667 amylopectin potato starch. Carbohyd. Polym. 57, 55-66.

668 Ortega-Toro, R., Jimenez, A., Talens, P., Chiralt, A., 2014. Properties of starch-hydroxypropyl
669 methylcellulose based films obtained by compression molding. Carbohyd. Polym. 109, 155-165.
670 Park, S., Chung, M.G., Yoo, B., 2004. Effect of octenylsuccinylation on rheological properties of corn starch
671 pastes. Starch-Starke. 56, 399-406.
672 Peressini, D., Bravin, B., Lapasin, R., Rizzotti, C., Sensidoni, A., 2003. Starch-methylcellulose based edible
673 films: rheological properties of film-forming dispersions. J. Food. Eng. 59, 25-32.
674 Ren, F., Yu, B., Dong, D., Hou, Z.-h., Cui, B., 2017. Rheological, thermal and microstructural properties of
675 whey protein isolate-modified cassava starch mixed gels at different pH values. Int. J. Food Sci. Tech. 52,
676 2445-2454.
677 Rosalina, I., Bhattacharya, M., 2002. Dynamic rheological measurements and analysis of starch gels.
678 Carbohyd. Polym. 48, 191-202.
679 Rosell, C.M., Yokoyama, W., Shoemaker, C., 2011. Rheology of different hydrocolloids-rice starch blends.
680 Effect of successive heating-cooling cycles. Carbohyd. Polym. 84, 373-382.
681 Schmitz, C.S., De Simas, K.N., Santos, K., Joao, J.J., Amboni, R.D.D.M.C., Amante, E.R., 2006. Cassava
682 starch functional properties by etherification-hydroxypropylation. Int. J. Food Sci. Tech. 41, 681-687.
683 Taguet, A., Bureau, M.N., Huneault, M.A., Favis, B.D., 2014. Toughening mechanisms in interfacially
684 modified HDPE/thermoplastic starch blends. Carbohyd. Polym. 114, 222-229.
685 Tajuddin, S., Xie, F., Nicholson, T.M., Liu, P., Halley, P.J., 2011. Rheological properties of thermoplastic
686 starch studied by multipass rheometer. Carbohyd. Polym. 83, 914-919.
687 Viriden, A., Larsson, A., Schagerlof, H., Wittgren, B., 2010. Model drug release from matrix tablets
688 composed of HPMC with different substituent heterogeneity. Int. J. Pharmaceut. 401, 60-67.
689 Wang, Y., Yu, L., Xie, F., Zhang, L., Liao, L., Liu, H., Chen, L., 2016a. Morphology and properties of
690 thermal/cooling-gel bi-phasic systems based on hydroxypropyl methylcellulose and hydroxypropyl starch.
691 Compos. Part B-Eng. 101, 46-52.
692 Wang, Y., Zhang, L., Liu, H., Yu, L., Simon, G.P., Zhang, N., Chen, L., 2016b. Relationship between
693 morphologies and mechanical properties of hydroxypropyl methylcellulose/hydroxypropyl starch blends.
694 Carbohydr Polym. 153, 329-335.

695 Woggum, T., Sirivongpaisal, P., Wittaya, T., 2015. Characteristics and properties of hydroxypropylated rice
696 starch based biodegradable films. Food Hydrocolloid. 50, 54-64.
697 Zhang, B., Chen, L., Zhao, Y., Li, X., 2013a. Structure and enzymatic resistivity of debranched high
698 temperature–pressure treated high-amylose corn starch. J. Cereal Sci. 57, 348-355.
699 Zhang, J., Yang, W., Vo, A.Q., Feng, X., Ye, X., Kim, D.W., Repka, M.A., 2017a. Hydroxypropyl
700 methylcellulose-based controlled release dosage by melt extrusion and 3D printing: Structure and drug release
701 correlation. Carbohyd. Polym. 177, 49-57.
702 Zhang, L., Wang, Y., Liu, H., Yu, L., Liu, X., Chen, L., Zhang, N., 2013b. Developing hydroxypropyl
703 methylcellulose/hydroxypropyl starch blends for use as capsule materials. Carbohyd. Polym. 98, 73-79.
704 Zhang, L., Wang, Y.F., Yu, L., Liu, H.S., Simon, G., Zhang, N.Z., Chen, L., 2015. Rheological and gel
705 properties of hydroxypropyl methylcellulose/hydroxypropyl starch blends. Colloid. Polym. Sci. 293, 229-237.
706 Zhang, L., Zhao, Y., Qian, J.-Y., Jiang, S., Liu, J., He, X.-L., 2017b. Relationship between multi-scale
707 structures and properties of photophobic films based on hydroxypropyl methylcellulose and monosodium
708 phosphate. Carbohyd. Polym. 174, 572-579.
709 Zhang, N., Liu, H., Yu, L., Liu, X., Zhang, L., Chen, L., Shanks, R., 2013c. Developing gelatin-starch blends
710 for use as capsule materials. Carbohyd. Polym. 92, 455-461.
711

Tables

Table 1. Flow behavior index (*n*), fluid consistency index (*K*) during increasing shear rate and the degree of structural recovery (DSR) after a certain recovery time for the solution of HPMC, HPSs with different MSs, and HPMC/HPS blends with the different HPSs at 25 °C.

Sample names	Increasing shear rate		DSR (%)		
	n	*K* (Pa·s^n)	10 s	60 s	250 s
A939	0.377±0.002[a]	82.1±0.14	35.64±2.78	38.00±2.58	33.32±3.24
A1081	0.471±0.004	32.0±0.98	27.89±0.60	32.34±0.62	28.63±0.51
A939-HPMC	0.778±0.002	3.1±0.03	18.42±0.50	18.92±0.50	17.73±0.48
A1081-HPMC	0.754±0.002	3.7±0.06	24.01±1.07	25.28±0.93	22.60±0.83
HPMC	0.923±0.006	1.1±0.02	85.65±1.29	88.44±0.64	91.63±0.53

[a] Mean ± standard deviation.

Table 2. n', n'', G_0' and G_0'' for the solution of HPMC, HPSs with different MSs, and HPMC/HPS blends with the different HPSs at 5 °C and 85 °C as determined from Eqs. (2) and (3).

Sample	T (°C)	n'	G_0'	R^2	n''	G_0''	R^2
G80	5	0.030±0.001[a]	12,5572±4,947	0.9912	0.157±0.009	4,802±393	0.9527
	85	0.122±0.012	86,930±12,709	0.9920	0.056±0.001	14,489±3,382	0.9528
A939	5	0.061±0.000	1,220±17	0.9805	0.313±0.002	70±2	0.9816
	85	0.299±0.001	32±1	0.9899	0.447±0.030	11±3	0.9999
A1081	5	0.083±0.001	315±6	0.9564	0.479±0.001	19±0	0.9956
	85	0.680±0.000	1±0	0.9955	0.673±0.000	1±0	0.9981
G80-HPMC	5	0.080±0.001	6,198±675	0.9723	0.370±0.002	449±17	0.9971
	85	0.071±0.009	4,083±256	0.9942	0.136±0.028	345±38	0.9371
A939-HPMC	5	0.159±0.000	233±2	0.9757	0.480±0.005	32±1	0.9962
	85	0.153±0.015	1,370±326	0.9979	0.241±0.009	246±85	0.9953
A1081-HPMC	5	0.232±0.001	58±0	0.9647	0.603±0.001	12±0	0.9983
	85	0.089±0.019	810±55	0.9969	0.175±0.019	95±22	0.9777
HPMC	5	1.404±0.025	0.04±0	0.9951	0.974±0.001	2.2±0	0.9999
	85	0.071±0.004	2,062±20	0.9957	0.102±0.007	204±5	0.9761

[a] Mean ± standard deviation.

Table 3. Fractal structure parameters of the films of HPMC, HPSs with different MSs, and HPMC/HPS blends with the different HPSs.

HPMC-HPS	Fractal dimension (*D*)		
	10:0	5:5	0:10
A939	2.36	2.20	2.60
A1081	2.36	1.84	1.57

Table 4. Tensile properties of the films of HPMC, HPSs with different MSs, and HPMC/HPS blends with the different HPSs at 25 °C.

Sample names	Young's modulus (MPa)	Tensile strength (MPa)	Elongation at break (%)
A939	518.59±20.31[a]	13.63±0.48	26.77±3.54
A1081	27.37±1.85	10.11±0.47	135.33±3.38
A939-HPMC	319.83±23.78	8.04±0.44	4.64±0.35
A1081-HPMC	235.02±9.97	9.14±0.46	20.35±2.14
HPMC	270.28±9.27	15.05±0.51	24.86±1.43

[a] Mean ± standard deviation.

Table 5. Oxygen permeability of the films of HPMC, HPSs with different MSs, and HPMC/HPS blends with the different HPSs at 25 °C.

Sample names	OP ($cc/m^2/day$)
A939	0.19±0.01[a]
A1081	0.64±0.00
A939-HPMC	70.74±0.62
A1081-HPMC	39.25±0.53
HPMC	261.62±4.8

[a] Mean ± standard deviation.